Vertical Beamforming in Intelligent Reflecting Surface-aided Cognitive Radio Networks

S. Fatemeh Zamanian, S. Mohammad Razavizadeh, and Qingqing Wu

***Abstract*—In this letter, we investigate joint application of intelligent reflecting surface (IRS) and vertical beamforming in cognitive radio networks (CRN). After properly modeling the network, an optimization problem is formed to jointly design the beamforming vector and tilt angle at the secondary base station (BS) as well as the phase shifts at the IRS with the objective of maximizing spectral efficiency of the secondary network. The optimization problem is non-convex; thus, we propose an efficient solution method for it. Numerical results show that adding an IRS and optimizing the radiation orientation, can significantly improve performance of the CRNs.**

***Index Terms*—Intelligent reflecting surface (IRS), Reconfigurable intelligent surface (RIS), vertical beamforming, tilt angle optimization, cognitive radio networks, three dimensional (3D) beamforming.**

I. Introduction

Recently, intelligent reflecting surface (IRS), also known as reconfigurable intelligent surface (RIS), has been considered as a key technology to manipulate the wireless propagation environment for achieving various objectives [1]. An IRS-aided network comprises a programmable meta-surface with massive reflecting elements that their phases are optimized in a way to improve some metrics such as interference reduction, security enhancement, and energy efficiency [2], [3].

On the other hand, another well-known technique for improving the spectrum usage in wireless channels is cognitive radio which has always been known as a promising candidate for evolving the wireless networks [4]. IRS technology can be used in the cognitive radio networks (CRN) for further improvement in spectrum efficiency. In [5], the authors maximized the achievable weighted sum rate of the secondary system in an IRS-aided multiple-input multiple-output (MIMO) CRN wherein the precoding vector of the secondary base station (SBS) and the phase shifts of the IRS were jointly optimized. Authors in [6] and [7] maximized the achievable rate of the secondary system in a single-IRS-assisted downlink multiple-input single-output (MISO) CRN and in a multi-IRS-assisted downlink MISO CRN through joint optimization of the beamforming of the secondary transmitter and the IRS's phases. A similar optimization approach was proposed in [8], [9] to address the resource allocation and spectrum sharing problems in the IRS-assisted CRNs. In [10], the problem of imperfect channel state information (CSI) was studied and a cascaded BS-IRS-user channel was considered for a robust beamforming design. In [11], it was illustrated how to equip CRNs with IRS to solve the security issue attributed to CRNs. In [12], IRS was used to enhance cell-edge users' quality while mitigating the intercell interference. A thorough survey on IRS can be found in [13].

In addition to the above technologies, three dimensional (3D) beamforming is another evolving technology in new generations of wireless networks in which the radiation pattern of the base station (BS) in the elevation and azimuth domains are carefully adjusted to improve signal reception at some desired locations [14]. Because of the low sensitivity of the radiation pattern to the azimuth angle, 3D beamforming usually leads to optimization of the tilt angle, and, therefore, is also known as the vertical beamforming [15]. Particularly, vertical beamforming is useful for improving different network metrics such as spectral and energy efficiencies and security [16]. Vertical beamforming can also be jointly used with the IRS technology for more improvement in the network performance. The authors in [17] contemplated a BS with 3D beamforming capability to provide more degrees of freedom in design and deployment of the IRS-assisted MISO networks.

In this letter, we show how the performance of a CRN is improved by equipping it with an IRS and vertical beamforming mechanism at the SBS. In this way, we first propose a system model including a primary base station (PBS), an SBS, and an IRS. While both BSs are equipped with multiple antennas, only the SBS has the capability of vertical beamforming. Then, we aim to maximize the spectral efficiency (SE) of the secondary network by jointly optimizing the beamforming vector and tilt angle at the SBS and the phase shifts at the IRS. The proposed joint optimization problem is non-convex and hence we propose an efficient method to solve it. Specifically, we utilize alternative optimization and semidefinite relaxation (SDR) techniques to iteratively optimize the variables. We further extend the results to the 3D beamforming case. Also, we calculate the complexity of our proposed method. Numerical results illustrate that the performance of the CRNs can considerably improve when the tilt angle radiates in the direction of the IRS, and also the SE of the system gets better when the number of reflecting elements of the IRS increases.

S. F. Zamanian and S. M. Razavizadeh are with the School of Electrical Engineering, Iran University of Science & Technology (IUST), Tehran 1684613114, Iran (e-mail: f zamanian@elec.iust.ac.ir; smrazavi@iust.ac.ir).

Q. Wu is with the State Key Laboratory of Internet of Things for Smart City, University of Macau, Macau, 999078, and also with the National Mobile Communications Research Laboratory, Southeast University, Nanjing 210096, China (email: qingqingwu@um.edu.mo). The work of Q. Wu was supported in part by the Macau Science and Technology Development Fund, Macau SAR, under Grant 0119/2020/A3 and under Grant 0108/2020/A, and the Guangdong NSF under Grant 2021A1515011900, and the Open Research Fund of National Mobile Communications Research Laboratory, Southeast University (No. 2021D15).

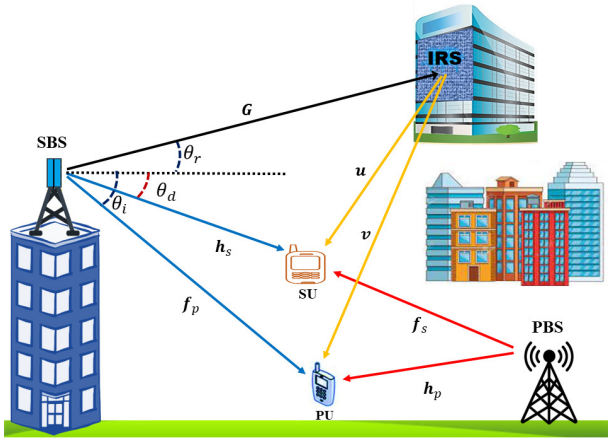

Figure 1. System model of the IRS-aided cognitive radio network.

II. System Model

As illustrated in Fig. 1, we consider the downlink transmission of an MISO CRN using underlay spectrum sharing. The primary system consists of a PBS equipped with N_p antennas that serves a single-antenna primary user (PU). Also, the secondary system consists of an SBS equipped with N_s antennas that serves a single-antenna secondary user (SU). Furthermore, an IRS comprising N reflecting elements is deployed to assist the secondary transmissions. The SBS is equipped with a full-dimensional array of antennas that adopts an optimized beamforming vector and tilt angle to transmit signals to its intended receivers with the help of the IRS. Because of the large distance between the PBS and IRS and also the obstacles between them, the link between them is ignored. In fact, in our scenario, we assume that the IRS is exploited only by the secondary system and it is placed in an appropriate position that mostly receives the secondary system's signals. Besides, we only consider the first-order reflection from the IRS due to the significant path loss.

In Fig. 1, $\mathbf{G} \in \mathbb{C}^{N \times N_s}$ denotes the channel matrix between the SBS and the IRS. Also, $\mathbf{v} \in \mathbb{C}^{N \times 1}$ and $\mathbf{u} \in \mathbb{C}^{N \times 1}$ are the channel vectors between the IRS and the PU and SU, respectively. In addition, $\mathbf{h}_p \in \mathbb{C}^{N_p \times 1}$ and $\mathbf{h}_s \in \mathbb{C}^{N_s \times 1}$ denote the channel vectors between the PBS and SBS and the PU and SU, respectively. Moreover, $\mathbf{f}_p \in \mathbb{C}^{N_s \times 1}$ and $\mathbf{f}_s \in \mathbb{C}^{N_p \times 1}$ are the interference channel vectors between the SBS and PBS and the PU and SU, respectively. We consider perfect channel state information (CSI) to reveal the theoretical gain obtained from equipping a CRN with IRS and 3D beamforming techniques [5]. However, in the numerical simulations in Sec. IV, we evaluate the impact of imperfect CSI on the performance of our proposed scheme and the results are shown.

Note that to employ vertical beamforming, we model the vertical antenna attenuation (pattern) at the SBS as follows [17]

$$a_V^x(\theta_{tilt}, \theta_x) = -min\left[12\left(\frac{\theta_x - \theta_{tilt}}{\theta_{3dB}}\right)^2, SLA_V\right], \quad (1)$$

where $x \in \{d, r, i\}$ and θ_d, θ_r and θ_i are the elevation angles of the SU, IRS and PU, respectively. Moreover, θ_{tilt} is the vertical tilt angle, θ_{3dB} is the vertical 3 dB beamwidth, and SLA_V is the maximum side-lobe level where it is usually assumed that $SLA_V = \infty$. Since θ_x is fixed for the given positions for the users and IRS, we define the vertical antenna attenuation (pattern) as $a_V^x(\theta_{tilt})$, or in linear scale as $A_V^x(\theta_{tilt}) = 10^{-1.2(\frac{\theta_x - \theta_{tilt}}{\theta_{3dB}})^2}$. Therefore, the received signals at the SU and PU are as follows, respectively

$$r_s = \underbrace{\sqrt{A_V^d(\theta_{tilt})}\mathbf{h}_s^H \mathbf{w}_s s_s}_{\text{direct link}} + \underbrace{\mathbf{f}_s^H \mathbf{w}_p s_p}_{\substack{\text{interference}\\ \text{link}}} + \underbrace{\mathbf{u}^H \mathbf{r}_r}_{\substack{\text{reflected}\\ \text{from IRS}}} + n_s, \quad (2)$$

$$r_p = \underbrace{\mathbf{h}_p^H \mathbf{w}_p s_p}_{\text{direct link}} + \underbrace{\sqrt{A_V^i(\theta_{tilt})}\mathbf{f}_p^H \mathbf{w}_s s_s}_{\substack{\text{interference}\\ \text{link}}} + \underbrace{\mathbf{v}^H \mathbf{r}_r}_{\substack{\text{reflected}\\ \text{from IRS}}} + n_p, \quad (3)$$

where

$$\mathbf{r}_r = \sqrt{A_V^r(\theta_{tilt})}\mathbf{\Phi}\mathbf{G}\mathbf{w}_s s_s, \quad (4)$$

and $\mathbf{\Phi} \triangleq \text{diag}(\phi) = \text{diag}(\phi_1, \phi_2, ..., \phi_N)$ is a diagonal matrix accounting for the effective phase shifts applied by all passive IRS reflecting elements, and $\phi_n = e^{j\alpha_n}$, $\forall n = 1, ..., N$[1]. Moreover, $\mathbf{w}_s$ and $\mathbf{w}_p$ are the beamforming vectors at the SBS and PBS, respectively. Also, s_s and s_p denote the normalized data signals transmitted by the SBS and PBS, respectively. Furthermore, n_s, $n_p \in \mathcal{CN}(0, \sigma_n^2)$ signify circularly-symmetric complex Gaussian noise at the SU and PU, respectively.

In this paper, we aim to maximize the SE of the secondary system. To this end, we first derive the SE of the secondary system in terms of the network parameters including the SBS tilt angle, beamforming vector and IRS phase shifts, and then maximize the SE through an optimization problem.

Specifically, based on (2), the signal-to-interference-plus-noise ratio (SINR) of the SU can be expressed as

$$SINR_s = \frac{\left|\left(\sqrt{A_V^d(\theta_{tilt})}\mathbf{h}_s^H + \sqrt{A_V^r(\theta_{tilt})}\mathbf{u}^H\mathbf{\Phi}\mathbf{G}\right)\mathbf{w}_s\right|^2}{\sigma_n^2 + |\mathbf{f}_s^H \mathbf{w}_p|^2}. \quad (5)$$

Then, the secondary SE is obtained as

$$SE_s = \log_2(1 + SINR_s). \quad (6)$$

According to the above, to maximize the SE_s, we formulate an optimization problem as follows

$$\begin{aligned} \max_{\mathbf{\Phi},\, \theta_{tilt},\, \mathbf{w}_s} \; & \log_2\left(1 + \frac{\left|\left(\sqrt{A_V^d(\theta_{tilt})}\mathbf{h}_s^H + \sqrt{A_V^r(\theta_{tilt})}\mathbf{u}^H\mathbf{\Phi}\mathbf{G}\right)\mathbf{w}_s\right|^2}{\sigma_n^2 + |\mathbf{f}_s^H \mathbf{w}_p|^2}\right) \\ s.t.\; & C_1: \left|\left(\sqrt{A_V^i(\theta_{tilt})}\mathbf{f}_p^H + \sqrt{A_V^r(\theta_{tilt})}\mathbf{v}^H\mathbf{\Phi}\mathbf{G}\right)\mathbf{w}_s\right|^2 \le \Gamma, \\ & C_2: |\phi_n|^2 = 1, \quad \forall n = 1, ..., N, \\ & C_3: \theta_{min} \le \theta_{tilt} \le \theta_{max}, \\ & C_4: ||\mathbf{w}_s||^2 \le P. \end{aligned} \quad (7)$$

[1]To maximize the signal reflection of the IRS, the reflection amplitude is set as one [1].

The constraints of (7) are as follows. C_1 guarantees the primary system interference condition, where Γ is the interference threshold of the primary network. Furthermore, C_2 is the IRS-gain constraint. Moreover, C_3 denotes the allowable interval of θ_{tilt}. Also, C_4 represents the power budget condition of the SBS where P is the maximum total power of the SBS.

The optimization variables in the objective function of problem (7) are coupled, thus, the objective function exhibits a non-convex form. Moreover, the left-hand side of constraint C_1 is a non-convex function and also the left-hand side of the equality constraint C_2 is nonlinear. Therefore, the problem (7) is a highly non-convex problem and it is difficult to find its optimal value in polynomial time. Accordingly, to solve it, we utilize SDR technique and propose an alternating method as follows.

III. Proposed Method

In this section, we propose an efficient solution method for (7). By ignoring the monotonic logarithm function and constant terms, we get an equivalent optimization problem as follows

$$\begin{aligned}
&\max_{\mathbf{\Phi},\, \theta_{tilt},\, \mathbf{w_s}} \left|\left(\sqrt{A_V^d(\theta_{tilt})}\mathbf{h}_s^H + \sqrt{A_V^r(\theta_{tilt})}\mathbf{u}^H\mathbf{\Phi}\mathbf{G}\right)\mathbf{w}_s\right|^2 \\
&s.t.\ C_1: \left|\left(\sqrt{A_V^i(\theta_{tilt})}\mathbf{f}_p^H + \sqrt{A_V^r(\theta_{tilt})}\mathbf{v}^H\mathbf{\Phi}\mathbf{G}\right)\mathbf{w}_s\right|^2 \le \Gamma, \\
&\quad C_2: |\phi_n|^2 = 1 \quad \forall n = 1, ..., N, \\
&\quad C_3: \theta_{min} \le \theta_{tilt} \le \theta_{max}, \\
&\quad C_4: ||\mathbf{w}_s||^2 \le P.
\end{aligned} \tag{8}$$

In the following, we first obtain the optimum value of θ_{tilt} with given $\mathbf{\Phi}$ and $\mathbf{w}_s$ and then optimize $\mathbf{w}_s$ with given $\mathbf{\Phi}$ and θ_{tilt}. After that, we obtain the optimum value of $\mathbf{\Phi}$ with given θ_{tilt} and $\mathbf{w}_s$, and we propose an alternating algorithm to solve (8). Finally, we analyze the computational complexity of our proposed method.

A. Optimizing θ_{tilt} with Given $\mathbf{\Phi}$ and $\mathbf{w}_s$

We firstly focus on the objective function of (8) to obtain the optimum value of θ_{tilt}, i.e. θ_{tilt}^*. Let us rewrite the objective function of (8) as follows

$$\left|10^{-0.6(\frac{\theta_d-\theta_{tilt}}{\theta_{3dB}})^2}\mathbf{h}_s^H\mathbf{w}_s + 10^{-0.6(\frac{\theta_r-\theta_{tilt}}{\theta_{3dB}})^2}\mathbf{u}^H\mathbf{\Phi}\mathbf{G}\mathbf{w}_s\right|^2. \tag{9}$$

It is not difficult to check that the curve of $10^{-0.6(\frac{\theta_x-\theta_{tilt}}{\theta_{3dB}})^2}$ has a unique maximum value at θ_x. Therefore, by assuming $\theta_r \neq \theta_d$, (9) has two extrema at θ_d and θ_r. Now, if $|\mathbf{h}_s^H\mathbf{w}_s| > |\mathbf{u}^H\mathbf{\Phi}\mathbf{G}\mathbf{w}_s|$, then $\theta_{tilt}^* = \theta_d$, and if $|\mathbf{h}_s^H\mathbf{w}_s| < |\mathbf{u}^H\mathbf{\Phi}\mathbf{G}\mathbf{w}_s|$, then $\theta_{tilt}^* = \theta_r$.

Due to the randomness of the channels, one way to find θ_{tilt}^* is to compare the expectation of $|\mathbf{h}_s^H\mathbf{w}_s|^2$ and $|\mathbf{u}^H\mathbf{\Phi}\mathbf{G}\mathbf{w}_s|^2$. Let us assume that all elements of the channels' $\mathbf{h}_s$, $\mathbf{u}$ and $\mathbf{G}$ have identically independent distributions of $\mathcal{CN}\left(0, \sigma_{\mathbf{h}_s}^2\right)$, $\mathcal{CN}\left(0, \sigma_{\mathbf{u}}^2\right)$, and $\mathcal{CN}\left(0, \sigma_{\mathbf{G}}^2\right)$, respectively. Then, we have

$$E\left[|\mathbf{h}_s^H\mathbf{w}_s|^2|\right] \overset{a}{=} \sigma_{\mathbf{h}_s}^2 Tr(\mathbf{w_s}\mathbf{w_s}^H) = \sigma_{\mathbf{h}_s}^2||\mathbf{w_s}||_2^2, \tag{10}$$

where $Tr(\cdot)$ stands for trace of matrix and $\overset{a}{=}$ is because of the following equalities

$$\begin{aligned}
&E\left[Tr\left(.\right)\right] = Tr\left(E\left[.\right]\right), \\
&Tr\left(\mathbf{AB}\right) = Tr\left(\mathbf{BA}\right).
\end{aligned} \tag{11}$$

Also

$$\begin{aligned}
&E\left[|\mathbf{u}^H\mathbf{\Phi}\mathbf{G}\mathbf{w}_s|^2\right] \overset{b}{=} \sigma_{\mathbf{u}}^2 Tr\left(E\left[\mathbf{\Phi}\mathbf{G}\mathbf{w}_s\mathbf{w}_s^H\mathbf{G}^H\mathbf{\Phi}^H\right]\right) \\
&\overset{c}{=} \sigma_{\mathbf{u}}^2 E\left[Tr\left(\mathbf{G}^H\mathbf{G}\mathbf{w}_s\mathbf{w}_s^H\right)\right] \overset{d}{=} \sigma_{\mathbf{u}}^2 Tr\left(E\left[\mathbf{G}^H\mathbf{G}\right]\mathbf{w}_s\mathbf{w}_s^H\right) \\
&= \sigma_{\mathbf{u}}^2 N\sigma_{\mathbf{G}}^2||\mathbf{w_s}||_2^2,
\end{aligned} \tag{12}$$

where $\overset{b}{=}$ is verified by (11) and also independent of $\mathbf{u}$ and $\mathbf{G}$, $\overset{c}{=}$ is due to $\mathbf{\Phi}^H\mathbf{\Phi} = \mathbf{I}_N$ and $\overset{d}{=}$ is due to $\mathbf{w}_s$ is deterministic in this subsection. When $\sigma_{\mathbf{u}}^2 N\sigma_{\mathbf{G}}^2||\mathbf{w_s}||_2^2 > \sigma_{\mathbf{h}_s}^2||\mathbf{w_s}||_2^2$, i.e. $N\sigma_{\mathbf{u}}^2\sigma_{\mathbf{G}}^2 > \sigma_{\mathbf{h}_s}^2$, we obtain $\theta_{tilt}^* = \theta_r$. This is the case for large enough values of N, which is usual in IRS technology. Moreover, for sufficiently large value of Γ, constraint C_1 of (8) will be satisfied for $\theta_{tilt}^* = \theta_r$. Our simulation results reveal that $N = 36$ and $\Gamma = 10^{-12}$ w satisfy the mentioned requirements.

It should be noted that, extending our results from tilt angle optimization to 3D beamforming, i.e. tilt and azimuth angles optimization, is straightforward. To elaborate, consider the overall SBS antenna gain in linear scale as

$$A^x(\theta_{tilt}, \phi_{azimuth}) = A_m 10^{-1.2\left[\left(\frac{\theta_x-\theta_{tilt}}{\theta_{3dB}}\right)^2 + \left(\frac{\phi_x-\phi_{azimuth}}{\phi_{3dB}}\right)^2\right]}, \tag{13}$$

where $x \in \{d, r, i\}$ and ϕ_d, ϕ_r and ϕ_i are the horizontal angles of the SU, IRS and PU, respectively. Moreover, $\phi_{azimuth}$ is the azimuth angle, ϕ_{3dB} is the horizontal 3 dB beamwidth, and A_m is the maximum directional gain of the antenna array elements. It is easy to verify optimizing ϕ_x is completely similar to that of θ_x and the optimal ϕ_x is ϕ_r. Therefore, the spectral efficiency of the secondary system improves when the tilt and azimuth angles orient towards the IRS.

B. Optimizing $\mathbf{w}_s$ with Given $\mathbf{\Phi}$ and θ_{tilt}

By fixing $\mathbf{\Phi}$ and θ_{tilt}, we need to solve the following sub-problem.

$$\begin{aligned}
&\max_{\mathbf{w_s}} \quad \mathbf{a}\mathbf{w}_s\mathbf{w}_s^H\mathbf{a}^H \\
&s.t. \quad \mathbf{b}\mathbf{w}_s\mathbf{w}_s^H\mathbf{b}^H \le \Gamma, \\
&\qquad ||\mathbf{w}_s||^2 \le P,
\end{aligned} \tag{14}$$

where $\mathbf{a} = \sqrt{A_V^d(\theta_{tilt})}\mathbf{h}_s^H + \sqrt{A_V^r(\theta_{tilt})}\mathbf{u}^H\mathbf{\Phi}\mathbf{G}$ and $\mathbf{b} = \sqrt{A_V^i(\theta_{tilt})}\mathbf{f}_p^H + \sqrt{A_V^r(\theta_{tilt})}\mathbf{v}^H\mathbf{\Phi}\mathbf{G}$. Then, by defining $\mathbf{W}_s = \mathbf{w}_s\mathbf{w}_s^H$, the optimization problem can be rewritten as

$$\begin{aligned}
&\max_{\mathbf{W}_s \succeq \mathbf{0}} \quad \mathbf{a}\mathbf{W}_s\mathbf{a}^H \\
&s.t. \quad \mathbf{b}\mathbf{W}_s\mathbf{b}^H \le \Gamma, \\
&\qquad \mathrm{tr}(\mathbf{W}_s) \le P, \\
&\qquad rank(\mathbf{W}_s) = 1.
\end{aligned} \tag{15}$$

This optimization problem is still non-convex. Thus, we use SDR technique by removing $rank(\mathbf{W}_s) = 1$ to transform it to a convex problem. Then, to address the relaxed constraint $rank(\mathbf{W}_s) = 1$, and to obtain solution to problem (15), we apply the sequential rank-one constraint relaxation (SROCR) technique [18].

Algorithm 1 Proposed Algorithm

1: **Requirement:** $\theta_r, \theta_d, \theta_i, N, N_s, P, \Gamma, \sigma_n$.
2: **Initialization:** $\mathbf{\Phi}^{(\mathbf{0})}$.
3: $\theta^*_{tilt} = \theta_r$.
4: $Err = \infty$.
5: **while** $Err \geq \epsilon$ **do**
6: Set $t = t + 1$.
7: With given $\mathbf{\Phi}^{(t-1)}$ solve problem (15), then apply SROCR technique over its solution to obtain $\mathbf{w}_s^{(t)}$.
8: With given $\mathbf{w}_s^{(t)}$ solve problem (19), then apply SROCR technique over its solution to obtain $\mathbf{\Phi}^{(t)}$.
9: Obtain $SE_s^{(t)}$ using (6).
10: $Err = \frac{SE_s^{(t)} - SE_s^{(t-1)}}{SE_s^{(t)}}$.

C. Optimizing $\mathbf{\Phi}$ with Given $\mathbf{w_s}$ and θ_{tilt}

In this section, by using $\mathbf{u}^H\mathbf{\Phi}\mathbf{G} = \phi^H \text{ diag}(\mathbf{u})\mathbf{G}$ and $\mathbf{v}^H\mathbf{\Phi}\mathbf{G} = \phi^H \text{ diag}(\mathbf{v})\mathbf{G}$ [2], we have the following sub-problem

$$\begin{aligned} \max_{\mathbf{x}} \quad & l_1 + \mathbf{x}^H\mathbf{H}_1\mathbf{x} \\ s.t. \quad & l_2 + \mathbf{x}^H\mathbf{H}_2\mathbf{x} \leq \Gamma, \\ & \text{diag}(\mathbf{x}\mathbf{x}^{\text{H}}) = \mathbf{1}, \end{aligned} \tag{16}$$

where $\mathbf{x} = [\phi^H \ , 1]^H$, $l_1 = A_V^d(\theta_{tilt})\mathbf{h}_s^H\mathbf{w}_s\mathbf{w}_s^H\mathbf{h}_s$ and $l_2 = A_V^i(\theta_{tilt})\mathbf{f}_p^H\mathbf{w}_s\mathbf{w}_s^H\mathbf{f}_p$. Also, $\mathbf{H}_1$ and $\mathbf{H}_2$ are given in (17) and (18), respectively, at the top of the next page.

Problem (16) is a non-convex problem, thus, we use semidefinite programming to solve it as follows.

$$\begin{aligned} \max_{\mathbf{X}\succeq\mathbf{0}} \quad & l_1 + \text{tr}(\mathbf{H}_1\mathbf{X}) \\ s.t. \quad & l_2 + \text{tr}(\mathbf{H}_2\mathbf{X}) \leq \Gamma, \\ & \text{diag}(\mathbf{X}) = \mathbf{1}, \\ & rank(\mathbf{X}) = 1, \end{aligned} \tag{19}$$

where $\mathbf{X} = \mathbf{x}\mathbf{x}^H$. Note that, $rank(\mathbf{X}) = 1$ in problem (19) is a non-convex constraint. Thus, we use SDR by simply removing $rank(\mathbf{X}) = 1$ to convexify (19). After that, we use SROCR to obtain an approximate solution to problem (19).

Remark: At each iteration of Algorithm 1, two maximization sub-problems (15) and (19) are solved using SROCR, for which local optimum solutions are obtained [18]. This means that the objective functions are non-decreasing. Moreover, the objective functions are bounded above due to Cauchy-Schwarz inequality, and hence the algorithm will converge.

D. Complexity of the Proposed Solution Method

The main complexity of Algorithm 1 is determined by steps 7 and 8. The complexity of these steps are $O((N_s+1)^{4.5})$ and $O((N+1)^{4.5})$, respectively [19]. Thus, the complexity of Algorithm 1 is approximately of $O\left(M\left((N_s+1)^{4.5}+(N+1)^{4.5}\right)\right)$, where M indicates the iteration number required for achieving convergence. Based on our simulations, M is usually less than 4 for an accuracy of $\epsilon = 10^{-3}$.

IV. Numerical Results

In this section, the performance of the proposed scheme is investigated. The parameters that we use are presented in Table I. We assume that the SBS, PBS, SU, PU, and IRS are located at $(90, 250, 40)$, $(0, 60, 20)$, $(390, 0, 3)$, $(30, 200, 3)$, $(80, 258, 46)$ in meter, in a three dimensional plane, respectively. We have generated all the channel coefficients $\mathbf{G}$, $\mathbf{u}$, $\mathbf{v}$, $\mathbf{h}_p$, $\mathbf{h}_s$, $\mathbf{f}_p$ and $\mathbf{f}_s$ using the relationship $\sqrt{\zeta_0(d_0/d)^\alpha}g_R$, where $\zeta_0 = -30dB$ is the path loss at the reference point $d_0 = 1\,m$, d denotes the distance between the source and the destination, α shows the path loss exponent, and g_R denotes the small scale fading component. Also, to model the small scale fading, we utilize Rician fading model with Rician factor $K = 1$. Furthermore, we consider noise power as $\sigma_n^2 = -100$ dBm. Moreover, we assume that $\mathbf{w}_p = \sqrt{P_p}\frac{\mathbf{h}_p}{||\mathbf{h}_p||}$, where P_p is the maximum total power of the PBS. Also, we use CVX toolbox of MATLAB to solve the resultant convex problems, and adopt the Monte Carlo method to obtain the results. The main parameters are listed in Table 1.

Table I
Parameters

Parameter	Value	Parameter	Value
θ_d	-5°	θ_r	25°
θ_i	-25°	θ_{3dB}	10°
θ_{min}	−60°	θ_{max}	60°
$\alpha_{\mathbf{v}}$	2.2	$\alpha_{\mathbf{f}_p}$	2.2
$\alpha_{\mathbf{u}}$	2	$\alpha_{\mathbf{f}_s}$	2
$\alpha_{\mathbf{G}}$	2.1	$\alpha_{\mathbf{h}_s}$	3.8
P_p	5 dBw	Γ	10^{-12} w

Fig. 2 shows the secondary spectral efficiency versus the vertical tilt angle (θ_{tilt}). It can be seen that when the vertical tilt angle (θ_{tilt}) is adjusted to be equal to the elevation angle of the IRS (θ_r), the maximum SE at the secondary system is achieved. In other words, the optimum value of θ_{tilt} is equal to θ_r. Also, another peak in the secondary SE occurs at θ_d shows that when there is no IRS in the network, the optimum value of θ_{tilt} is equal to θ_d. However, in this case, the achievable SE is lower than the case that IRS is used. Besides, we can see that increasing the number of antennas at the SBS (N_s) enhances the secondary spectral efficiency.

Fig. 3 depicts the secondary spectral efficiency versus the number of reflecting elements of the IRS (N) at either the optimum value of θ_{tilt} obtained from Fig. 2 or arbitray values $\theta_{tilt} = \theta_d$ and random θ_{tilt}. It is observed that the SE of the proposed IRS phase optimization method is higher than a scheme with random and fixed phase shifts at the IRS. Also, it is observed that the SE always increases with N only for the optimum θ_{tilt} and is fixed for the other θ_{tilt}'s. Moreover, by increasing N, the gap between the "proposed method", and other methods becomes larger, which shows that our proposed method is particularly effective for larger N.

Fig. 4 illustrates that the spectral efficiency of the secondary system improves when the secondary system has a large maximum allowed total power (P). In addition, we can see that the system equipped with the IRS has better performance than the system with no IRS at all SBS powers. Finally, the impact of imperfect CSI on the performance of our scheme is evaluated and shown in this figure. Imperfect CSI is obtained by adding a random Gaussian value to each element of the channel matrix. The results show a degradation in the performance, however it still satisfactory.

V. Conclusion

In this letter, we investigated vertical beamforming in an IRS-aided CRN. We formulated a maximization problem to improve the secondary spectral efficiency, and then proposed an efficient method to solve it. Numerical results showed that the network performance improves when the SBS orientation is towards the IRS and also when the IRS is equipped with a large number of reflecting elements.

References

[1] Q. Wu and R. Zhang, "Intelligent reflecting surface enhanced wireless network via joint active and passive beamforming," IEEE Trans. Wireless Commun., vol. 18, no. 11, pp. 5394-5409, Nov. 2019.

[2] Q. Wu and R. Zhang, "Beamforming optimization for wireless network aided by intelligent reflecting surface with discrete phase shifts," IEEE Trans. Commun., vol. 68, no. 3, pp. 1838–1851, Mar. 2020.

$$\mathbf{H}_1 = \begin{bmatrix} A_V^r(\theta_{tilt})\mathrm{diag}(\mathbf{u})\mathbf{G}\mathbf{W}_s\mathbf{G}^{\mathrm{H}}\mathrm{diag}(\mathbf{u}) & \sqrt{A_V^r(\theta_{tilt})A_V^d(\theta_{tilt})}\mathrm{diag}(\mathbf{u})\mathbf{G}\mathbf{W}_s\mathbf{h}_s \\ \sqrt{A_V^r(\theta_{tilt})A_V^d(\theta_{tilt})}\mathbf{h}_s^H\mathbf{W}_s\mathbf{G}^H\mathrm{diag}(\mathbf{u}) & 0 \end{bmatrix} \tag{17}$$

$$\mathbf{H}_2 = \begin{bmatrix} A_V^r(\theta_{tilt})\mathrm{diag}(\mathbf{v})\mathbf{G}\mathbf{W}_s\mathbf{G}^{\mathrm{H}}\mathrm{diag}(\mathbf{v}) & \sqrt{A_V^r(\theta_{tilt})A_V^i(\theta_{tilt})}\mathrm{diag}(\mathbf{v})\mathbf{G}\mathbf{W}_s\mathbf{f}_p \\ \sqrt{A_V^r(\theta_{tilt})A_V^i(\theta_{tilt})}\mathbf{f}_p^H\mathbf{W}_s\mathbf{G}^H\mathrm{diag}(\mathbf{v}) & 0 \end{bmatrix} \tag{18}$$

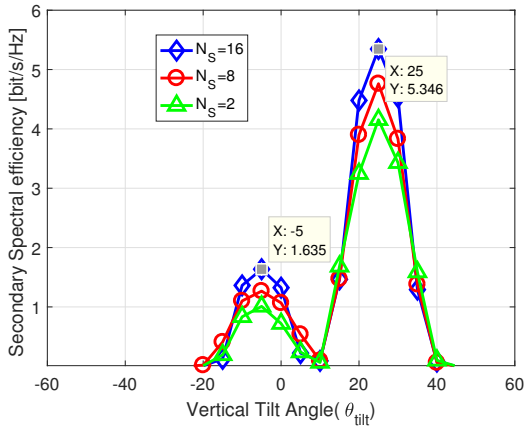

Figure 2. Secondary spectral efficiency versus the vertical tilt angle (θ_{tilt}) in different values of the number of antennas at the SBS (N_s) (with $P = 10dBw$ and $N = 36$).

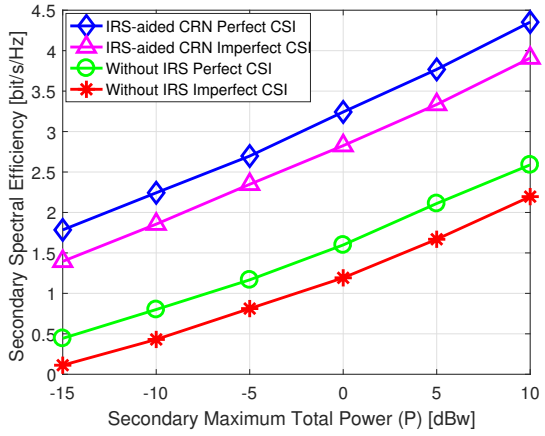

Figure 4. Secondary spectral efficiency versus the secondary maximum allowed total power (P) (with $N_s = 4$, $N = 36$ and optimized tilt angle).

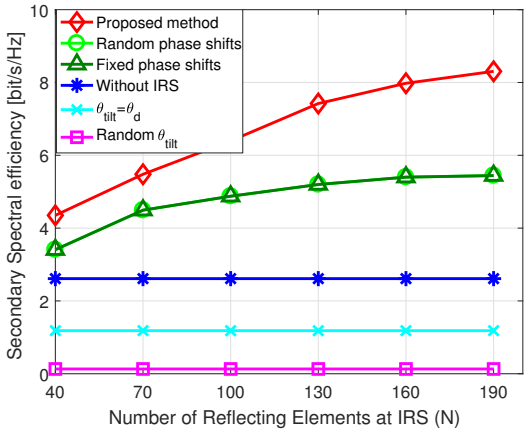

Figure 3. Secondary spectral efficiency versus the number of IRS elements (N) (with $P = 10dBw$, $N_s = 2$).

[3] Q. Wu and R. Zhang, "Towards smart and reconfigurable environment: Intelligent reflecting surface aided wireless network," IEEE Commun. Mag., vol. 58, no. 1, pp. 106-112, Jan. 2020.

[4] F. Hu, B. Chen and K. Zhu, "Full Spectrum Sharing in Cognitive Radio Networks Toward 5G: A Survey," IEEE Access, vol. 6, pp. 15754-15776, Feb. 2018.

[5] L. Zhang, Y. Wang, W. Tao, Z. Jia, T. Song and C. Pan, "Intelligent Reflecting Surface Aided MIMO Cognitive Radio Systems," IEEE Trans. Veh. Technol., vol. 69, no. 10, pp. 11445-11457, Oct. 2020.

[6] J. Yuan, Y. Liang, J. Joung, G. Feng and E. G. Larsson, "Intelligent Reflecting Surface -Enhanced Cognitive Radio System," IEEE International Conf. on Commun. (ICC), Dublin, Ireland, 2020, pp. 1-6.

[8] D. Xu, X. Yu, Y. Sun, D. W. K. Ng and R. Schober, "Resource Allocation for IRS-assisted Full-Duplex Cognitive Radio Systems," IEEE Trans. Commun, vol. 68, no. 12, pp. 7376-7394, Dec. 2020.

[7] J. Yuan, Y. -C. Liang, J. Joung, G. Feng and E. G. Larsson, "Intelligent Reflecting Surface-Assisted Cognitive Radio System," IEEE Trans. Commun., vol. 69, no. 1, pp. 675-687, Jan. 2021.

[9] X. Guan, Q. Wu, and R. Zhang, "Joint power control and passive beamforming in IRS-assisted spectrum sharing," IEEE Commun. Lett., vol. 24, no. 7, pp. 1153–1157, Jul. 2020.

[10] L. Zhang, C. Pan, Y. Wang, H. Ren, K. Wang, and A. Nallanathan, "Robust beamforming design for intelligent reflecting surface aided cognitive radio systems with imperfect cascaded CSI," arXiv preprint:2004.04595, 2020.

[11] H. Xiao, L. Dong, and W. Wang, "Intelligent reflecting surface-assisted secure multi-input single-output cognitive radio transmission," Sensors (Switzerland), vol. 20, no. 12, pp. 1–23, Jun. 2020.

[12] C. Pan, H. Ren, K. Wang, W. Xu, M. Elkashlan, A. Nallanathan, and L. Hanzo, (2020). "Multicell MIMO communications relying on intelligent reflecting surfaces " IEEE Trans. Wireless Comm.vol. 19, no. 8, pp. 5218-5233, Aug. 2020.

[13] R. Nandana, et al., "White paper on broadband connectivity in 6G," arXiv preprint arXiv:2004.14247, 2020.

[14] S. M. Razavizadeh, M. Ahn and I. Lee, "Three-Dimensional Beamforming: A new enabling technology for 5G wireless networks," IEEE Signal Process. Mag., vol. 31, no. 6, pp. 94-101, Nov. 2014.

[15] W. Lee, S. Lee, H. Kong, S. Lee and I. Lee, "Downlink Vertical Beamforming Designs for Active Antenna Systems," IEEE Trans. Commu., vol. 62, no. 6, pp. 1897-1907, Jun. 2014.

[16] Q. Nadeem, A. Kammoun, and M. Alouini, "Elevation Beamforming With Full Dimension MIMO Architectures in 5G Systems: A Tutorial," IEEE Commun. Surveys & Tutorials, vol. 21, no. 4, pp. 3238-3273, Jul. 2019.

[17] S. M. Razavizadeh and T. Svensson, "3D Beamforming in Reconfigurable Intelligent Surfaces-assisted Wireless Communication Networks," WSA 2020; 24th International ITG Workshop on Smart Antennas, Hamburg, Germany, 2020, pp. 1-5.

[18] P. Cao, J. Thompson, and H. V. Poor, "A sequential constraint relaxation algorithm for rank-one constrained problems," in Proc. Eur. Signal Process. Conf. (EUSIPCO), pp. 1060-1064, 2017.

[19] Z. Luo, W. Ma, A. M. So, Y. Ye and S. Zhang, "Semidefinite Relaxation of Quadratic Optimization Problems," IEEE Signal Process. Mag., vol. 27, no. 3, pp. 20-34, May. 2010.